molecular pharmaceutics

pubs.acs.org/molecularpharmaceutics

Article

Flow Activation Energy of High-Concentration Monoclonal Antibody Solutions and Protein−Protein Interactions Influenced by NaCl and Sucrose

Guangcui Yuan,* Paul F. Salipante, Steven D. Hudson, Richard E. Gillilan, Qingqiu Huang, Harold W. Hatch, Vincent K. Shen, Alexander V. Grishaev, Suzette Pabit, Rahul Upadhya, Sudeep Adhikari, Jainik Panchal,* Marco A. Blanco,* and Yun Liu*

Cite This: *Mol. Pharmaceutics* 2024, 21, 4553−4564

Read Online

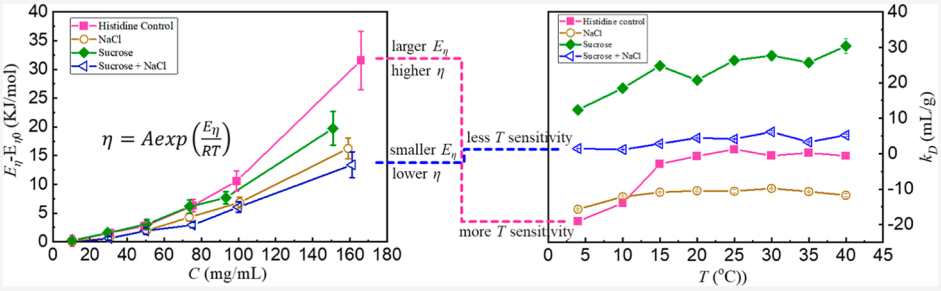

ABSTRACT: The solution viscosity and protein−protein interactions (PPIs) as a function of temperature (4−40 °C) were measured at a series of protein concentrations for a monoclonal antibody (mAb) with different formulation conditions, which include NaCl and sucrose. The flow activation energy (E_η) was extracted from the temperature dependence of solution viscosity using the Arrhenius equation. PPIs were quantified via the protein diffusion interaction parameter (k_D) measured by dynamic light scattering, together with the osmotic second virial coefficient and the structure factor obtained through small-angle X-ray scattering. Both viscosity and PPIs were found to vary with the formulation conditions. Adding NaCl introduces an attractive interaction but leads to a significant reduction in the viscosity. However, adding sucrose enhances an overall repulsive effect and leads to a slight decrease in viscosity. Thus, the averaged (attractive or repulsive) PPI information is not a good indicator of viscosity at high protein concentrations for the mAb studied here. Instead, a correlation based on the temperature dependence of viscosity (i.e., E_η) and the temperature sensitivity in PPIs was observed for this specific mAb. When k_D is more sensitive to the temperature variation, it corresponds to a larger value of E_η and thus a higher viscosity in concentrated protein solutions. When k_D is less sensitive to temperature change, it corresponds to a smaller value of E_η and thus a lower viscosity at high protein concentrations. Rather than the absolute value of PPIs at a given temperature, our results show that the temperature sensitivity of PPIs may be a more useful metric for predicting issues with high viscosity of concentrated solutions. In addition, we also demonstrate that caution is required in choosing a proper protein concentration range to extract k_D. In some excipient conditions studied here, the appropriate protein concentration range needs to be less than 4 mg/mL, remarkably lower than the typical concentration range used in the literature.

KEYWORDS: *monoclonal antibody, protein interactions, viscosity, NaCl, sucrose, dynamic light scattering, small-angle X-ray scattering, rheology, temperature sensitivity, flow activation energy*

■ INTRODUCTION

Monoclonal antibodies (mAbs) are a fast-growing group of pharmaceutical molecules[1,2] The mAb solutions usually exhibit peculiar and diverse viscosity−concentration profiles that the viscosity increases in an exponential manner with increasing antibody concentration. This behavior is of significant interest because the rise in viscosity will pose challenges in manufacturing, administration, and delivery.[2−4] In order to develop general strategies and guidelines to select low-viscosity candidates at early drug discovery stages, there have been considerable efforts focusing on understanding the key factors controlling the viscosity of concentrated mAb solutions.[3−15] The discussion of concentration-dependent viscosity behavior often falls into a colloidal description of protein solutions that relies predominantly on pairwise intermolecular interactions.

Received: April 26, 2024
Revised: August 12, 2024
Accepted: August 13, 2024
Published: August 20, 2024

Under such a framework, elevated viscosities are generally linked to protein−protein interactions (PPIs), which change with distance (therefore concentration) and relative protein orientations, leading to non-ideal solution behaviors. There have been many efforts to investigate the potential correlation between the quantifiers of PPIs and measured viscosity.[16−18]

Experimental determination of the orientation influence on anisotropic PPIs, such as the PPIs among mAbs, has been a long-standing challenge. Commonly used parameters to characterize PPIs, such as the second virial coefficient (B_{22}) or the diffusion interaction parameter (k_D), are the averaged results over protein orientations and distances and are measured at low protein concentrations.[19] The sign and magnitude of B_{22} or k_D represent the sum of all underlying interactions (e.g., electrostatic interactions, van der Waals interactions, hydrogen bonds, and hydrophobic interactions) that can exist between mAbs. Several techniques can be used to measure B_{22}, including osmometry,[20] static light[19,21,22]/X-ray[23,24]/neutron[25] scattering, sedimentation equilibrium,[26] self-interaction chromatography,[27] and size-exclusion chromatography.[28] The parameter k_D can be obtained by dynamic light scattering (DLS) using the approximately linear relationship of diffusion coefficient (D) vs concentration (C).[29] Values of k_D reflect both thermodynamic and hydrodynamic interactions. A linear correlation between B_{22} and k_D has been reported for a substantial number of measurements[16−18,30−32] at a wide range of solution conditions (pH and ionic strength) and many mAbs. Since the measurement of B_{22} can be cumbersome and time-consuming, and k_D can be determined by DLS with a high-throughput and small quantities of proteins, there is a growing trend of using k_D as an indicator of PPIs. In some reports, deviations from the linear dependence between B_{22} and k_D could also be found,[13,33] especially when a relatively large quantity of excipients, such as sugars, was added. Caution is required to explicitly consider the presence of such a solute and its self- and hetero-interactions.

It has been proposed that k_D (or B_{22}) can be reasonably utilized for the viscosity prediction for different mAbs in the same formulation; i.e., samples with positive k_D values generally tend to have lower solution viscosity at high concentrations, whereas negative k_D values are linked to higher viscosity. This proposal is consistent with an intuitive physical picture that attractive PPIs may introduce reversible cluster formation, driving the viscosity higher.[4,14,15,34−37] In fact, the analysis of a diverse database (29 mAbs in Connolly et al.'s work[17] and 59 mAbs in Kingsbury et al.'s work[18]) seems to indicate that this proposal can be a reasonable approach. However, results from some other mAbs have not always agreed with this proposal. For instance, Yadav et al.[3] demonstrated a case that k_D of a mAb-A is more negative, indicating relatively stronger attractions in dilute solution as compared with mAb-H, but mAb-H is more viscous than mAb-A at high protein concentrations. Moreover, when comparing mAb solutions in different formulations, the value of k_D (or B_{22}) does not always correlate well with the viscosity.[13,32,34,38−42] If using only the value of k_D (or B_{22}) as an indicator of PPIs, one will find in some cases that even large and qualitative changes in PPIs caused by excipients do not result in a significant change in solution viscosity, while in other cases, increased viscosity can be caused by both increased k_D and decreased k_D, as shown in Woldeyes et al.'s[32] work on 4 different mAbs under a range of formulation conditions (i.e., pH and/or ionic strength). This inconsistency illustrates the limitation of predicting (quantitatively in particular) the high concentration behaviors by the results from dilute solutions, further highlights the complex nature of the PPI−viscosity relation, and raises the question about the validity of using the value of k_D (or B_{22}) as a predictor of the viscosity behavior of concentrated protein solutions. Since k_D (or B_{22}) offers only averaged interaction information obtained at relatively dilute conditions, it is not very surprising that k_D (or B_{22}) may not be able to explain the properties at high concentrations for some proteins.

Temperature is another factor altering PPIs and solution viscosity, which has not been extensively investigated. The temperature dependency of quantities that characterize effective PPIs (i.e., B_{22} or k_D) is influenced by the formulation conditions and proteins because PPIs depend on the interplay between proteins and solvent molecules.[43−46] And the solution viscosity of many mAbs[11,36,47−49] and globular proteins[37,50,51] has been generally observed to decrease with increasing temperature. However, to the best of our knowledge, very few studies have been reported to explore the change of PPIs as a function of temperature and its relationship with viscosity for mAb systems. Recently, Woldeyes et al.[47] studied the temperature effect on the viscosity of 3 proteins including 2 mAbs, at different pH values and ionic strengths, and discussed the concentration−temperature−viscosity−PPI relations. The sensitivity of viscosity to temperature can be described in terms of an Arrhenius activation energy of viscous flow (E_η), which assesses the minimum energy required for a molecule of the solution to escape the influence of its neighbor molecules. They found that E_η, which is a function of concentration, is sensitive to the types of proteins but is independent of the studied formulations. The larger E_η is associated with the higher viscosity of the concentrated solutions. They also suggested that the anisotropic attractive interactions, which are sensitive to temperature, account for the highest rise in viscosity at high protein concentrations.

However, it is not clear if Woldeyes et al.'s[47] observations can be applied to other mAbs and different types of formulations. Because of the huge diversity in mAb molecules, it is thus necessary to explore other mAb systems with additional formulation conditions. The objective of this work is to examine the correspondence in temperature dependence of PPIs and solution viscosity of an industrial mAb and its impacts by NaCl and sucrose. The IgG1 mAb obtained from Merck & Co., Inc. (Rahway, NJ, USA) has a net charge of +17 at pH 6. According to the predictions from a work using machine learning by Lai et al.,[8] the viscosity of mAb with the net charge between 12 and 34 is not only determined by charge effects but also partly correlated with the hydrophilic and hydrophobic residues in the Fv regions of mAb. Here, a common salt NaCl which is generally known to screen electrostatic interactions and a popularly used tonicity modifier sucrose which stabilizes proteins by preferential exclusion and hydration model as explained by Timasheff and Lee[52,53] were chosen as excipients for the purpose of this study. The impacts of NaCl and sucrose, separately and together, help to identify the nature of dominated interactions. A correlation based on the temperature dependence of viscosity (i.e., E_η) and the temperature sensitivity in PPIs was observed. The information presented in this study will be beneficial for the development of a more efficient formulation design methodology.

https://doi.org/10.1021/acs.molpharmaceut.4c00460
Mol. Pharmaceutics 2024, 21, 4553−4564

METHODS

Sample Preparation. Buffers were prepared in distilled, deionized water (resistivity 18.2 MΩ cm, Millipore): (i) pH 6.0, 10 mM histidine; (ii) pH 6.0, 10 mM histidine with added 150 mM NaCl; (iii) pH 6.0, 10 mM histidine with added 70 mg/mL sucrose; (iv) pH 6.0, 10 mM histidine with added 150 mM sodium chloride and 70 mg/mL sucrose. All buffers were filtered through a 0.22 μm PES filter (Thermo Fisher Scientific) and stored at 4 °C prior to further use. The initial 25 mg/mL mAb solutions in 20 mM sodium citrate buffer at pH 6.0 with 150 mM NaCl (as received from Merck & Co., Inc., Rahway, NJ, USA) were dialyzed into the buffers described above, respectively. To ensure a complete buffer exchange, a 10 mL starting mAb solution in Slide-A-Lyzer Dialysis Cassettes (10 kDa MWCO, Thermo Fisher Scientific) was dialyzed against 1000 mL of the desired buffer using three 12 h buffer exchanges at 4 °C. The dialyzed mAb solution was then sterile-filtered with a 0.22 μm PES filter. For each formulation condition, a series of protein solutions with concentrations covered from 1 to 160 mg/mL were prepared. Concentrated protein solutions were obtained using 30 kDa MWCO ultracentrifugal filter units (Millipore) through membrane centrifugation at 4500*g*. Concentrations of mAb solutions were measured by a NanoDrop One^C UV−vis spectrometer (Thermo Fisher Scientific) using an extinction coefficient of 1.64 mL mg^{-1} cm^{-1}. The concentration value (C) used in this study was the mean value based on 5 replicates. The standard deviation of C was within ±2% for $C \leq 50$ mg/mL and ±5% for $C > 50$ mg/mL.

Microcapillary Viscosity. Viscosity measurements were conducted using a small-volume microcapillary rheometer developed by Salipante et al.[54] Liquid samples (∼150 μL) were driven pneumatically through a microcapillary and partially filled a larger glass capillary with a diameter of 100 μm. The glass capillary was mounted on an optical linear sensor to track the air−liquid meniscus in real time and trigger the reversal of the flow direction by switching a pneumatic valve. Each transit provided a volumetric flow rate measurement, which was used with the pressure drop to determine the viscosity as a function of the shear rate. A given sample was measured over at least 2−3 decades in shear rate, in the range of 10−10^5 s^{-1}. Temperature sweeps (at 4, 10, 20, 30, and 40 °C) were conducted in situ for each sample. A 5 min thermal equilibration was allowed before each measurement. All measured solutions demonstrated a Newtonian fluid response; i.e., the viscosity was independent of the measured shear rate. Viscosity was averaged over all shear rates measured with an estimated uncertainty within ±5%.

Dynamic Light Scattering. Assessment of the interaction parameter k_D was performed using DLS at 4, 10, 15, 20, 25, 30, 35, and 40 °C using a Dynapro Nanostar instrument (Wyatt) with a scattering angle of 90°. Fifteen minutes were allowed for thermal equilibration at the targeted temperature. Samples were filtered through a 0.22 μm PES filter before the DLS measurement. A total of 20 scans of 30 s each were recorded and analyzed, and results were averaged for each measurement. The regularization method was used to calculate the collective diffusion coefficient D from the intensity autocorrelation function ($G^2(t)$). The concentration dependence of D was used to calculate k_D and the infinite-dilution diffusion coefficient (D_0) as a function of temperature according to

$$D = D_0(1 + k_D C) \tag{1}$$

The presented results of D are mean values with standard error determined in triplicate for each protein concentration. In sufficiently dilute systems, the average hydrodynamic radius (R_h) can be calculated from its D using the Stokes−Einstein−Sutherland equation

$$D = \frac{k_B T}{6\pi\eta_b R_h} \tag{2}$$

where k_B is the Boltzmann constant, T is the temperature, and η_b is the buffer viscosity. The influence of 150 mM NaCl on the solvent viscosity is considered to be negligible based on the viscosity table of aqueous NaCl solutions provided by Kestin et al.,[55] so is the influence of 10 mM histidine due to its very low concentration. The viscosity of the 70 mg/mL sucrose solution at different temperatures was calculated based on the available data and method described by Telis et al.[56] Values for buffer viscosity used in this study are listed in the Supporting Information. The effect of temperature-dependent reduction of the refractive index was insignificant within the studied temperature range based on the findings of Schiebener et al.,[57] and no temperature corrections of the refractive index were made.

Small-Angle X-ray Scattering. The second virial coefficients (B_{22}) of mAbs were analyzed by small-angle X-ray scattering (SAXS). Measurements were performed at the ID-7A1 Bio-SAXS beamline at the Cornell high-energy synchrotron source. This instrument employed a photon energy of ≈9.8 keV with 1.5% bandwidth, had a sample-to-detector distance of 1648 mm, and probed scattering wavevector, Q, values of 0.008−0.52 Å^{-1}. Measurements were conducted at 4, 20, and 40 °C. The sample chamber was a capillary that oscillated the 50 μL sample back and forth to minimize the damage from radiation. Each measurement was made by exposing the oscillating sample to the beam at least 5 times (up to 100 times for low-concentration solutions such as C = 1 mg/mL) of 1 or 0.5 s per exposure. Exposures indicating no radiation damage were then averaged together to improve counting statistics. Data reduction was performed using BioXTAS RAW software.[58] Background subtraction for capillary and corresponding buffers were performed.

SAXS intensity for a simple, noncompressible system consisting of monodisperse scattering particles in a solvent can be generally expressed as

$$I(Q) = N_A(C/M)(\Delta\rho)^2 V^2 P(Q) S(Q) \tag{3}$$

in which V is the molecular volume of the particles (here proteins), (C/M) is the molar concentration of proteins, and $\Delta\rho$ is the difference in the scattering length density between proteins and the solvent. In addition, $P(Q)$ is the normalized form factor that represents the shape of the scattering objects, which is unity in the limit-of-zero scattering angle, and $S(Q)$ is the structure factor that takes into account the effects of thermodynamic nonideality arising from the PPI, which is approximately unity at low particle concentrations where the interparticle interference is negligible.

The accessible low-Q limit corresponds to R = 78.5 nm ($=2\pi/Q_{min}$) in real space; therefore, part of the Q-range satisfying the criteria $QR < 1.3$ (with $R \approx 5.0$ nm) is available for Guinier approximation.[59] Extrapolation of the intensity to zero scattering angle using Guinier approximation[59] yields $I(0)$

$$\ln I(Q) = \ln I(0) - (R_g^2/3)Q^2 \tag{4}$$

https://doi.org/10.1021/acs.molpharmaceut.4c00460
Mol. Pharmaceutics 2024, 21, 4553−4564

Here, R_g is the radius of gyration. Substitution of a value of unity for $P(Q)$ in eq 3 then gives

$$I(0) = N_A(C/M)(\Delta\rho)^2V^2S(0) \quad (5)$$

For convenience, eq 5 is rearranged as

$$\frac{C}{I(0)} = \frac{M}{N_A(\Delta\rho)^2V^2S(0)} = \frac{1}{KS(0)} \quad (6)$$

Combination of eq 6 with the relationship

$$S(0) = 1/(1 + 2B_{22}C + ...) \quad (7)$$

for the description of thermodynamic nonideality then leads to the expression[60]

$$\frac{C}{I(0)} = \frac{1 + 2B_{22}C + ...}{K} \approx \frac{1}{K} + \frac{2B_{22}C}{K} \quad (8)$$

SAXS experiments were performed on a series of mAb concentrations for each excipient formulation. Equation 8 allows quantification of B_{22} (mL mol g^{-2}) from the slope/ordinate intercept ratio of a linear dependence of $C/I(0)$ upon C. Here, a concentration region of 1−7.5 mg/mL was subjected to B_{22} calculation.

With concentration increases, SAXS profiles reflected contributions from both $P(Q)$ and $S(Q)$. Compared to the SAXS profiles measured from dilute solutions, where PPIs were minimal, the appearance of $S(Q)$ was reflected by the deviation of $I(Q)$ at a low scattering angle. Experimentally, $S(Q)$ was calculated by comparing the concentration-normalized scattering intensity at low and high concentrations

$$S(Q) = \frac{I(Q, C)/C}{I(Q, C_{dilute})/C_{dilute}} \quad (9)$$

Here, the experimentally determined structure factor is defined as "effective" $S(Q)$ because it is affected by the shape and anisotropy of interactions between molecules. In this study, C_{dilute} is ∼1 mg/mL.

■ RESULTS

Viscosity of mAb Solutions. The results of viscosity measurement are summarized in Figure 1 as functions of protein concentration and temperature for the 4 sets of formulation conditions studied. Relative viscosity (η_r) is defined as the ratio between the total viscosity of mAb solutions (η) and the corresponding buffer viscosity (η_b) at the measured temperature. Because η_r is normalized by the solvent viscosity, the change of η_r as a function of the temperature is thus mainly driven by the change of the equilibrium structures formed by proteins and controlled by the protein concentration and PPIs.[4] The values of η_r are observed to increase with increasing protein concentration under all 4 formulation conditions. This is expected because there are more transient bindings between proteins in solutions with increasing concentration.

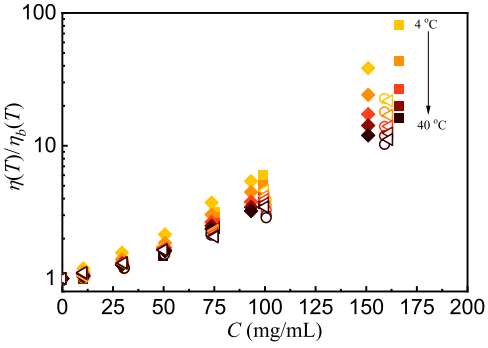

Figure 1. Temperature effect on solution viscosity as a function of concentration under 4 different excipient conditions: (■) histidine control; (○) NaCl; (♦) sucrose; (◁) sucrose + NaCl. For a given concentration in all samples, the viscosity values follow a decreasing trend as temperature increases (color darkens from 4, 10, 20, 30, and 40 °C) indicated by the arrow.

Adding NaCl effectively decreases η_r. Adding sucrose shows relatively less reduction on η_r. Samples with lower ionic strength, i.e., in histidine control and with sucrose-added conditions, have consistently higher viscosity as compared to samples with NaCl added. The solution viscosity of the highest concentration measured (∼160 mg/mL) at 20 °C is 27 cP in the histidine control condition and 13 cP with 150 mM NaCl added, respectively. Note that adding NaCl can reduce[11,12,32,34] or increase[13,18,35,41] viscosities or have no effect on the viscosity[10,32,34,35,40] in published reports. The difference is claimed to be related to the different dependencies of PPIs on ionic strength.[4] Sucrose has also been reported to reduce[2,41,61] or increase[11,13,42,61] the solution viscosity, or has no effect,[61] depending on the nature of given mAbs. Despite the large body of work examining the effects of excipients, there are currently no methods yet to predict NaCl and sucrose actions on a given mAb. Note that the pharmaceutically desirable limit for subcutaneous injection is ∼20 cP at the target dose concentration, above which the protein solutions can be difficult to inject.[2]

With an increase in temperature, η_r decreases for all samples, as indicated by the downward arrow in Figure 1. The relative change of the viscosity by temperature is larger for solutions without added NaCl than those with added NaCl. When the temperature increases from 4 to 40 °C, the viscosity at ∼160 mg/mL decreases from 127 to 10 cP for the sample in histidine control buffer, which is by a factor of about 13. However, the viscosity for the sample in a buffer with 150 mM NaCl changes from 35 to 7 cP within the same temperature range, which is by a factor of 5. This is a sign of change in PPIs which will be discussed later in the paper.

The impact of temperature on the solution viscosity can be examined quantitatively by extracting the effective E_η using an empirical Arrhenius-type model

$$\eta = A\exp\left(\frac{E_\eta}{RT}\right) \quad (10)$$

where the pre-exponential term (A) is related to an activation entropy and E_η is the apparent activation energy of viscous flow.[62,63] By taking the natural log of each side of eq 10, a linear relationship between ln η and $1/T$ was used to calculate E_η and ln A. Because the activation energy includes the contributions of both the solvents and the proteins, the activation energy of the whole solution (E_η) is subtracted by the activation energy of the solvent (E_0). Thus, ($E_\eta - E_0$) is mainly influenced by the interactions between proteins. Figure 2 shows ($E_\eta - E_0$) as a function of mAb concentration under 4 different excipient conditions. It is evident that ($E_\eta - E_0$) increases as a function of concentration. In the case of hard spheres, the increased solution viscosity at higher concentrations is completely due to packing effects, where the

https://doi.org/10.1021/acs.molpharmaceut.4c00460
Mol. Pharmaceutics 2024, 21, 4553−4564

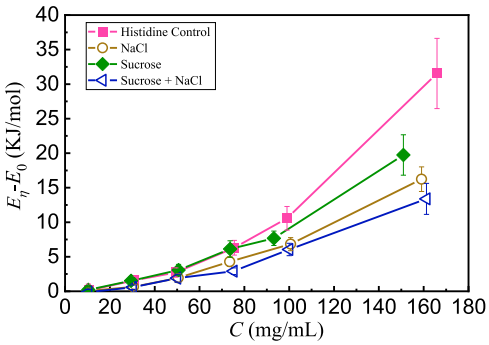

Figure 2. Arrhenius activation energy of solution viscosity (E_η) with the solvent contribution (E_0) subtracted as a function of protein concentration in 4 different excipient conditions. Error bars represent standard errors from the computation.

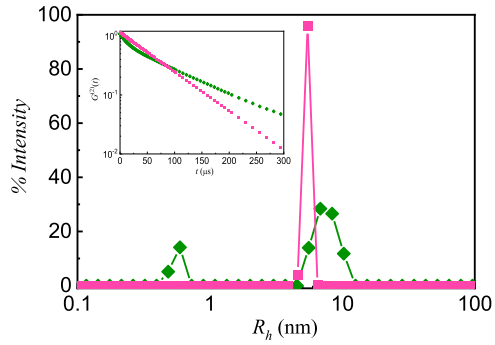

Figure 3. R_h distribution function of two solutions with sucrose (♦) and without sucrose (■) at a mAb concentration of ∼1 mg/mL. The measured temperature is 4 °C. Inset is the corresponding intensity−intensity time correlation function.

apparent E_η as a function of concentration is expected to be a constant. This constant E_η behavior has been observed for a globular protein previously.[47] Here, the gradual increase of E_η values as a function of concentration indicates that additional PPIs, besides the colloidal crowding effect, play a central role in viscosity increase at higher mAb concentrations.

In the previous study by Woldeyes et al.,[47] it was observed that $(E_\eta - E_0)$ at a given concentration is independent of the formulation conditions (pH and ionic strength) but determined by the type of proteins only. Interestingly, for the mAb studied here, the extracted $(E_\eta - E_0)$ values vary with the excipient conditions. Meanwhile, $(A_\eta - A_0)$ seems to be independent of the buffer conditions within the statistical uncertainty, as shown in the Supporting Information. Therefore, according to eq 10, a higher value of E_η should correspond to higher viscosity in the given formulations. In Figure 2, samples in the histidine control show the largest E_η, which corresponds to the highest increases in viscosity at high protein concentrations. Adding NaCl results in smaller E_η, which corresponds to less increases in viscosity at high protein concentrations. Overall, viscosity refers to a fluid's resistance to flow. Activation energy is like the energy needed to kickstart a process. Activation energy influences fluid viscosity. Higher activation energy means higher viscosity, while lower activation energy leads to lower viscosity. In the following, we will look for the relationship between the sensitivity of viscosity to temperature (E_η) and the temperature dependence of PPIs.

DLS Results. To understand the PPI and its change as a function of temperature, DLS experiments were conducted under 4 different excipient conditions. It is important to note that the values of D and thus R_h are affected by both the mAb and the buffer conditions due to the inherently multi-component nature of these solutions. A typical set of correlation functions ($G_2(t)$) obtained by DLS and their corresponding best fits for hydrodynamic radius distributions using exponential functions are shown in Figure 3. There is no sign of aggregation in all of the DLS-measured samples. For solutions without added sucrose, the data can be well fit by a single relaxation mode, whereas for solutions with added sucrose, there is an additional fast decay, which requires a double-exponential fit. The fast-decaying mode is due to the fluctuation of sucrose added to the solution. The slow decaying mode is due to the motion of proteins in solution with sucrose. As discussed in the Methods section, care has been taken to consider the change of the solvent viscosity and refractive index when extracting the hydrodynamic radius, R_h. The extracted R_h for the mAb increased by about 1 nm after the addition of sucrose in the solution. This apparent increase of the protein size could be due to a corresponding increase in the thickness of the hydration layer around a protein, similar to what has been found in Baek et al.'s report.[42]

To illustrate the different effects of excipients and temperature on D, values of D for samples in a concentration range of 0.5−15 mg/mL, measured at 4, 20, and 40 °C, are shown in Figure 4A−C, respectively. The first thing to note is the opposite effects on the concentration dependence of D caused by NaCl and sucrose. For the samples added with NaCl, D decreases as a function of the protein concentration in the dilute region. For the samples added with sucrose, D increases as a function of the protein concentration in the very dilute region. For samples with both NaCl and sucrose added, D remains almost constant with an increasing protein concentration. This observation indicates that NaCl and sucrose change the overall PPI in different ways. Due to the increase of the solvent viscosity with added excipients (NaCl and sucrose), the values of D at (near-) zero concentration are relatively lower in various degrees as compared to the control group.

Similarly, due to the reduced solvent viscosity at elevated temperatures, an overall increase of D with increasing temperature is also noticed. Furthermore, increasing temperature causes various degrees of changes in the slope of D vs C, depending on the added excipients. A striking example is for samples in the histidine control condition. At 4 °C (Figure 4A), the entire concentration range with $C \leq 10$ mg/mL can be taken as a linear region with a negative slope. However, with an increase in temperature to 20 °C (Figure 4B), a linear model could not be applied over the same concentration range. Instead, this concentration range breaks down into two regions, one with a near-zero slope ($C < 4$ mg/mL) and the rest with a negative slope, as represented by the solid and dashed lines from the linear regressions, respectively. With increasing temperature, the plateau region with a near-zero slope gradually expands, and it extends to ∼8 mg/mL when the temperature reaches 40 °C (Figure 4C). The temperature impact on the concentration range of the linear portion is also noticeable in samples with added sucrose at low ionic strength (no added NaCl). Although positive slopes are observed at all measured temperatures, the linear portion in the D vs C plots shrinks from $C < 8$ mg/mL at 4 °C (Figure 4A) to $C < 5$ mg/mL at 40 °C (Figure 4C). The variation of the linear concentration range is less sensitive to temperature for samples

https://doi.org/10.1021/acs.molpharmaceut.4c00460
Mol. Pharmaceutics 2024, 21, 4553−4564

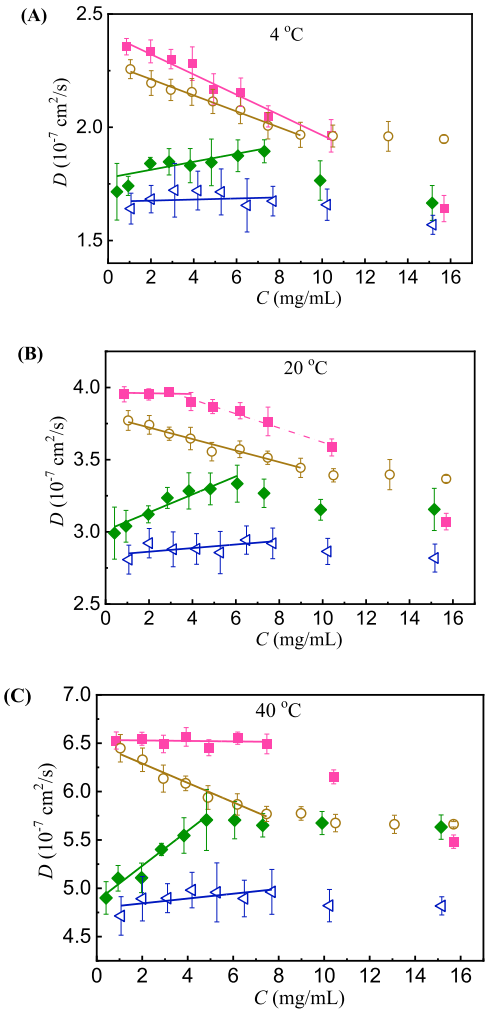

Figure 4. Concentration dependence of the diffusion coefficient of mAb solutions under 4 different excipient conditions at 3 temperatures: (A) 4 °C; (B) 20 °C, and (C) 40 °C; (■) histidine control; (○) NaCl; (♦) sucrose; (◁) sucrose + NaCl. Lines show the linear fit of D vs C. Error bars represent standard deviation from replicated measurements.

with NaCl added, regardless of sucrose, indicating that the cause of temperature sensitivity is electrostatic-related.

These observations not only demonstrate the different effects of excipient conditions and temperature on D but also highlight the challenges in extracting k_D accurately. The eq 1 used to extract k_D is based on a linear approximation when the concentration is small enough. With increasing concentration, the thermodynamic nonidealities, crowding effects, and higher-order interactions can alter net interactions, collective behavior can be dramatically different from that observed under dilute conditions.[64] In general, to calculate k_D from D vs C, 4−6 samples are typically measured with equally spaced protein concentration in a dilute region. Theoretically speaking, the smaller the protein concentration range used to extract k_D, the better the approximation. However, if the protein concentration is too small, the DLS signal may become noisy and sometimes influenced by the buffer molecules. Thus, from the signal intensity perspective of the DLS measurement, using larger protein concentrations is desired. Therefore, there is an optimal range one needs to choose to balance both factors. The protein concentration range commonly employed in the literature for linear fit is ≤12 mg/mL[3,5,16,32,33] or ≤25 mg/mL.[13,17,31,39,40,44] Even though the choice of concentration seems to be simple and straightforward, this is nontrivial in our cases. In some formulation conditions, such as the control sample at 20 °C (Figure 4B), D is apparently not a linear function of C at a concentration as low as about 4 mg/mL. The concentration range of ≤4 mg/mL is much smaller than the typical concentration range used in many literature reports. Here, the linear portions of the D vs C curves are chosen by visually inspecting the graphs and selecting only those data points that appear to lie on a straight line. The narrow range for linear extrapolation is due to the intrinsic nonlinearity of the D vs C curves at low ionic strength.[64] When no NaCl is added, the electrostatic interaction, which is typically long-ranged, dominates the PPIs in low-concentration regions. The calculation over the different concentration ranges could lead to large discrepancies in extracted k_D values. Our approach to improve accuracy is by reducing the spacing between data points by measuring more samples with smaller concentration increments. It is also interesting to see from our results that the temperature-sweep measurement helps to justify the proper linear portion. This is because the temperature-sweep measurements generate a series of D vs C plots for the same set of samples. In the case which may provoke controversy due to data fluctuation at the signal-to-noise ratio, the general trend observed in a sequence of temperatures can be used as a reference and guide our selection for the linear region. The D vs C data of all temperatures measured are available in the Supporting Information.

The calculated k_D values as a function of temperature in all 4 sets of excipient conditions are plotted in Figure 5. In general,

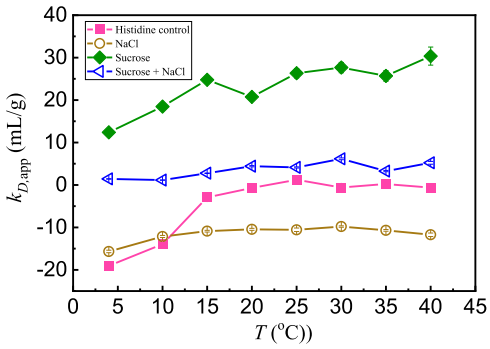

Figure 5. Temperature dependence of k_D of mAb solutions under 4 different excipient conditions. Error bars represent standard errors from the computation.

positive values for k_D represent repulsive intermolecular interactions and negative values represent attraction. Adding NaCl or sucrose shows opposite effects on the values of k_D. NaCl can screen the electrostatic repulsion, causing a dramatic decrease of k_D values as compared to the control group. Sucrose increases overall repulsion, causing a significant increase of the k_D values. This is consistent with the physical picture that adding sucrose can help form a hydration layer of water around a protein.[52,53] This hydration layer essentially increases the excluded volume of a protein to increase the k_D.

Adding NaCl or sucrose also shows opposite effects on the temperature sensitivity of k_D. For the sample in the histidine control condition, there is a steep increase in k_D when T increases from 4 to 15 °C, and it remains almost constant with T further increased to 40 °C. Thus, the mAb in this

https://doi.org/10.1021/acs.molpharmaceut.4c00460
Mol. Pharmaceutics 2024, 21, 4553−4564

formulation condition has an overall more attractive PPI at 4 °C than that at higher temperatures. Some other proteins also show stronger attraction at lower temperatures, such as lysozyme.[37] The origin of this temperature-dependent attraction has not been fully understood.[65] One speculation is that the temperature-sensitive attraction is often related to the hydrophobic patches on proteins. A similar temperature-dependent attraction is also observed when sucrose is added to the solution in our samples. Sucrose, which is known to alter the hydration property, has little impact on the temperature-sensitive attractions of the PPIs. Meanwhile, there is no obvious temperature dependence of k_D for samples with 150 mM NaCl. In general, salts can screen the electrostatic repulsion but are not expected to influence the hydrophobic introduced attraction between proteins. Therefore, this interesting temperature-dependent attraction is likely coupled with the charge interaction. Some future studies are needed to study the mutual influence between the charge distribution and potentially hydrophobic introduced attraction.

PPI Assessment by SAXS. There are many reports to compare the values between B_{22} and k_D.[13,16−18,30−32] Following eqs 4−8 discussed in the Methods section, B_{22} is extracted from the SAXS data. The values of B_{22} from SAXS data, as well as k_D from the DLS data, for samples at 20 °C are shown in Figure 6. It is noted that contrary to the extreme

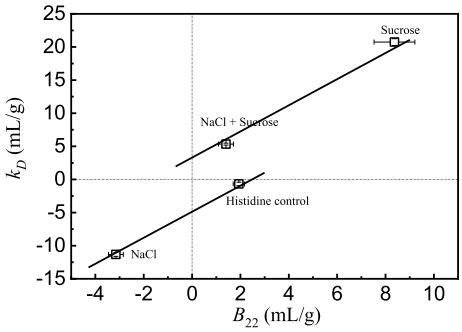

Figure 6. Plot containing correlation of k_D with B_{22} values for 4 excipient conditions measured at 20 °C. Two solid lines are references with slope = 2. Error bars represent standard errors from the computation.

sensitivity in the linearity of the D vs C curves at the dilute range for k_D calculation under some formulation conditions as discussed in the previous section, the SAXS $C/I(0)$ vs C curves for B_{22} calculation follow relatively excellent linearity in the dilute region (1−7.5 mg/mL) for all conditions. Illustrative examples of the regression of the SAXS data are shown in the Supporting Information.

Parameter B_{22} is determined by the effective PPI. In Figure 6, the B_{22} value in the histidine control buffer is slightly positive, suggesting a very weakly repulsive PPI. The effects of NaCl and sucrose on B_{22} are opposite to each other. Adding NaCl changes the interaction significantly, as B_{22} reduces to a negative value, suggesting an overall attractive PPI. Adding sucrose changes the interaction dramatically as well because B_{22} increases to a much more positive value, suggesting a stronger repulsive behavior. When adding both NaCl and sucrose, with NaCl decreasing the repulsive interaction by screening the long-ranged electrostatic interaction while sucrose increasing the repulsive interaction by introducing a potential hydration layer, the combined effect leads to no obvious change of B_{22} values compared to the control condition.

Parameter k_D is influenced by both the effective PPI and the hydrodynamic interactions. The diffusion coefficient can be expressed as[66]

$$D = D_0 \frac{H(Q=0)}{S(Q=0)} \tag{11}$$

where the hydrodynamic function $H(Q = 0)$ can be expanded at relatively dilute concentrations to

$$H(Q=0) = 1 + k_H C \tag{12}$$

k_H is the hydrodynamic term which is strongly influenced by the type of PPIs.[67−71] Combining this relationship with eqs 7 and 1 leads to

$$k_D = k_H + 2B_{22} \tag{13}$$

The two solid lines in Figure 6 are references with a slope = 2. The intercepts correspond to k_H. It is clear that k_H varies a lot between conditions with and without sucrose, which indicates that sucrose has a strong effect on the hydrodynamic flow. However, adding NaCl to the control samples or adding NaCl to the samples with sucrose shows little change to the intercept, i.e., k_H. Therefore, NaCl has little effect on the hydrodynamic flow. The change of k_D when adding NaCl is mainly due to the change of B_{22}, while the change of k_D when adding sucrose comes from both the B_{22} and the k_H.

At a given (especially high) protein concentration, $S(Q)$ is a straightforward characterization of PPI. The value of $S(Q = 0)$ is equal to the osmotic compressibility. When it is lower than unity, it signifies a repulsive interaction. An upturn at the low-Q part of $S(Q)$ signifies attractive interaction. Examples of $S(Q)$ from an intermediate concentration C = 50 mg/mL under different excipient conditions are shown in Figure 7A. It is clear that NaCl and sucrose have different effects on the overall interaction due to the difference at the low-Q part. Adding NaCl increases the low-Q part of $S(Q)$, indicating an overall weakening of the repulsion, while adding sucrose lowers the low-Q part of $S(Q)$, indicating an overall enhancement of repulsion. This observation is consistent with the k_D and B_{22} measurements. Additional differences caused by NaCl and sucrose can be seen from the first peak at $Q \approx 0.05$ A^{-1}. As compared to the control group, the presence of NaCl induces a closer and less regularly packed structure between neighboring proteins as indicated by the right shift of the peak with decreased peak intensity. The presence of sucrose does not alter the first interaction peak; thus, adding sucrose has little impact on the packing of the nearest neighboring proteins.

Figure 7B shows the $S(Q)$ of the control sample under 3 temperatures. Lowering the temperature from 20 to 4 °C leads to an overall upturn of the low-Q part, which is an indication of enhanced attraction at low temperatures and consistent with the k_D measurements. When the temperature is increased from 20 to 40 °C, it is seen at this intermediate concentration C = 50 mg/mL that the low-Q part of $S(Q)$ decreases, implying that the attraction becomes weaker at high temperatures. This is not reflected in the k_D results. The k_D obtained from DLS measurement remains at almost a constant value between 20 and 40 °C, indicating that the overall average PPI in dilute solutions does not change. This comparison shows that the extracted k_D values at low protein concentrations do not comprehensively reflect the actual situation at high protein

https://doi.org/10.1021/acs.molpharmaceut.4c00460
Mol. Pharmaceutics 2024, 21, 4553−4564

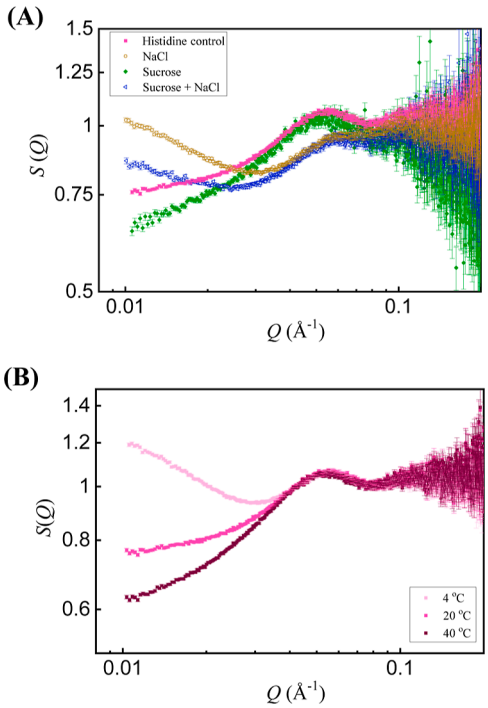

Figure 7. (A) Formulation dependence of $S(Q)$ measured at 20 °C; (B) temperature dependence of $S(Q)$ in the histidine control condition. The mAb concentration is C = 50 mg/mL.

concentrations. One other important observation from Figure 7B is that the first peaks of $S(Q)$ remain almost identical during the temperature change. Thus, the local packing of the proteins is not influenced by the temperature change. Overall, the studies of temperature dependence using SAXS provide rich information about the nature of the PPIs among proteins. Temperature effects on the scattering profiles of different formulation conditions are shown in the Supporting Information. The observations are consistent with the DLS and viscosity data that samples without NaCl show significant temperature-induced changes, but samples with NaCl are less sensitive to temperature.

■ DISCUSSION

The results measured by individual techniques are discussed above. Here, all of the measurement results are combined to gain a better understanding of the PPIs measured at different temperatures and their relationship with the viscosity.

First, we evaluate the relationship between the viscosity and PPIs of the mAb solutions for a given temperature (e.g., 20 °C). Four types of buffers were used to prepare protein samples: (i) pH 6.0, 10 mM histidine; (ii) pH 6.0, 10 mM histidine with added 150 mM NaCl; (iii) pH 6.0, 10 mM histidine with added 70 mg/mL sucrose; (iv) pH 6.0, 10 mM histidine with added 150 mM NaCl and 70 mg/mL sucrose. Formulation conditions influence both viscosity and the PPIs. The relative viscosity shown in Figure 1 basically is separated into two groups. Samples without NaCl, (i) and (iii), show relatively large viscosity. Samples with NaCl, (ii) and (iv), show relatively low viscosity. The rank order of the relative viscosity for all four samples at room temperature is (ii) ≈ (iv) < (iii) ≈ (i). This does not correlate well with the measured k_D (or B_{22}). The rank order of the measured k_D (or B_{22}) value from the most negative to the most positive at 20 °C is (ii) < (i) < (iv) < (iii). The sample with the most negative k_D value shows the lowest relative viscosity. The sample with the second most negative k_D value shows the highest relative viscosity. Thus, the average PPI information reflected by k_D (or B_{22}) is not a good indicator of viscosity at high protein concentrations for the studied mAb here.

Next, we establish the correspondence between the viscosity and the PPIs based on their temperature dependence because the excipient conditions influence the temperature dependence of viscosity and that of PPIs as well. The temperature sensitivity in viscosity is quantified in terms of E_η. A larger value of E_η corresponds to a greater change in η vs T. It correlates very well with the temperature sensitivity in k_D vs T as shown in Figure 5. A larger value of E_η corresponds to a greater change in k_D vs T. There are clearly steep increases in k_D when T is increased under conditions without NaCl added. Adding NaCl significantly represses the temperature sensitivity of k_D and the value of E_η. Therefore, the high-throughput DLS measurement at different temperatures should be vital because the variation of k_D vs T could have implications on E_η and thus viscosity.

Then, we discuss the cause of the failure in correlating the value of k_D (or B_{22}) with the viscosity in our cases by SAXS measurements of structure factors at relatively higher concentrations. It cannot be overemphasized that k_D (or B_{22}) represents the average of all underlying interactions. It is very possible that two different underlying mechanisms bring out the same apparent net effect. For instance, in our case, lowering the temperature to 4 °C in the histidine control condition and adding NaCl both give rise to a net attraction, as indicated by the almost identical negative k_D value (Figure 5). However, the structure factors (Figure 7) reveal that the underlying mechanisms are different. In the histidine control condition, most neighboring proteins remain effectively repulsive, as indicated by the first peak in the $S(Q)$ profile shown in Figure 7. In this case, a significantly smaller fraction of all possible orientations, i.e., anisotropic attractive interaction which has very large attractive energies, presumably dominates the net attraction. This anisotropic attraction is also the cause of the significant rise of viscosity at high concentrations. Proteins bind each other under certain orientations and form reversible clusters. The activation energy after subtracting that of the buffer, $E_\eta - E_0$, is determined by the energy needed to break the binding among moving protein units during a shearing force. Therefore, stronger anisotropy binding is linked to a larger value of the activation energy. The anisotropic interaction originates from the uneven distributions of the hydrophilic/hydrophobic surfaces. Note that only the hydrophilic surface is charged. Even though the apparent net charge is positive, uneven distributions of the charged surfaces can induce an overall attractive interaction. When NaCl is added, as indicated by the first peak in the $S(Q)$ profile, all electrostatic interaction is screened, including the electrostatic interactions between neighboring proteins and the anisotropic attraction between orientated proteins. By decreasing the strong binding strength, adding NaCl significantly lowers the activation energy.

Last, we point out that the information provided by k_D vs T can help to select viscosity candidates. Experimentally, the measurement of PPI, quantified in terms of k_D (or B_{22}), as a function of temperature can be used to assess certain conditions where anisotropic strong attractions would dominate the solution behavior and lead to evaluated viscosity.

https://doi.org/10.1021/acs.molpharmaceut.4c00460
Mol. Pharmaceutics 2024, 21, 4553−4564

Roberts and Blanco[72] examined the role of inherently anisotropic interactions on PPI expressions and tested the temperature effects by using a simple patchy model. They[72] found that, when a significantly smaller fraction of all possible orientations which have very large attractive energies dominates the net attraction, a small change in temperature causes overall PPIs to change dramatically. It seems from our results that a dramatic change in k_D from a small change in temperature (here 4−15 °C) could be a simple experimental means to identify this type of anisotropic attraction. To fully predict viscosity at high protein concentrations, it is important to find the binding strength of the specific orientations that contribute to the equilibrium protein structures. The average PPI information, such as k_D and B_{22}, may not necessarily have the same formulation dependence as the PPI at the relevant orientations and thus may not predict the viscosity at high concentrations for certain proteins. But the temperature dependence of PPI information could help to identify the difference. It is thus expected that molecular dynamics simulation may help to extract the orientation dependence so that it can be better correlated with the extracted activation energy, which will need to be studied further in the future.

■ CONCLUSIONS

Predicting the protein viscosity is a challenging problem for mAb-based therapeutic drugs. In the early stages of developing high-concentration biopharmaceutical formulations, experimental material is often limited. Screening tools, such as high-throughput and low-volume techniques (DLS), which help assess viscosity without extensive experimental studies, become essential to guide formulation decisions. The present work systematically investigated the viscosity and PPIs of a mAb at different formulation conditions and temperatures (ranging from 4 to 40 °C). The viscosity was measured from about 10 to about 160 mg/mL, and the activation energy of viscous flow was extracted from the temperature dependence of solution viscosity. The PPIs were evaluated by measuring k_D with the DLS, B_{22}, and the effective $S(Q)$ using SAXS.

It is found that the PPIs measured by DLS and SAXS are consistent with each other. There is a direct relationship between k_D and B_{22}. Adding NaCl decreases k_D (and B_{22}) as it screens the long-range electrostatic repulsion. Adding sucrose significantly increases k_D (and B_{22}) due to hydration repulsion. The value of k_D (and B_{22}) reflects only the interaction information averaged over all orientations and distances between neighboring proteins, but $S(Q)$ provides additional details of the interaction between neighboring proteins. Without NaCl, the interaction between neighboring proteins is repulsive.

It is also found that the viscosity measurements are consistent with the PPI results, regarding their temperature dependence. Samples without NaCl show significant temperature-induced changes, but samples with NaCl are less sensitive to the temperature. The value of k_D is not a good indicator to predict the viscosity of our mAb at high concentrations, but its temperature sensitivity is. A correlation between the viscosity and k_D based on their temperature sensitivity is established. When the net-PPIs are more sensitive to the temperature variation, it corresponds to a larger value of E_η and thus higher viscosity at high protein concentrations. When the net-PPIs are the least sensitive to temperature change, it corresponds to a smaller value of E_η and thus a lower viscosity at high protein concentrations. Currently, common practice to investigate issues with high solution viscosity is only at a single temperature, typically between 20 and 25 °C. Based on this finding, we suggest researchers in formulation design pay attention to the temperature sensitivity of k_D. Measuring k_D and viscosity at different temperatures allows us to gain more insight into the nature of PPIs. Further studies are underway to assess the applicability of this discovery in other protein systems.

■ ASSOCIATED CONTENT

Supporting Information

The Supporting Information is available free of charge at https://pubs.acs.org/doi/10.1021/acs.molpharmaceut.4c00460.

Values for buffer viscosity at different measured temperatures; calculation of error propagation; ln η vs $1/T$ plots for all measured solutions; effective activation entropy $(A_\eta - A_0)$ as a function of concentration in 4 formulation conditions; diffusion coefficient D vs C at all measured temperatures (4−40 °C); calculated hydrodynamic radius $(R_{h,0})$ as a function of temperature in 4 different formulation conditions; SAXS $I(Q)$ vs Q profiles for solutions in a concentration range of 1−100 mg/mL; SAXS Guinier plot ln I vs Q^2 for dilution solutions (1−7.5 mg/mL); SAXS $C/I(0)$ vs C curves for B_{22} calculation; and temperature effects (20 and 40 °C) on SAXS $I(Q)$ vs Q profiles for $C \approx 50$ mg/mL (PDF)

■ AUTHOR INFORMATION

Corresponding Authors

Guangcui Yuan − *Center for Neutron Research, National Institute of Standards and Technology, Gaithersburg, Maryland 20899, United States;* orcid.org/0000-0003-0063-3767; Email: guangcui.yuan@nist.gov

Jainik Panchal − *Sterile and Specialty Products, Merck & Co., Inc., Kenilworth, New Jersey 07033, United States;* Email: jainik.panchal@merck.com

Marco A. Blanco − *Discovery Pharmaceutical Sciences, Merck & Co., Inc., West Point, Pennsylvania 19486, United States;* Email: marco.blanco@merck.com

Yun Liu − *Center for Neutron Research, National Institute of Standards and Technology, Gaithersburg, Maryland 20899, United States; Department of Chemical and Biomolecular Engineering, University of Delaware, Newark, Delaware 19716, United States;* orcid.org/0000-0002-0944-3153; Email: yun.liu@nist.gov

Authors

Paul F. Salipante − *Materials Science and Engineering Division, National Institute of Standards and Technology, Gaithersburg, Maryland 20899, United States;* orcid.org/0000-0002-8692-4268

Steven D. Hudson − *Materials Science and Engineering Division, National Institute of Standards and Technology, Gaithersburg, Maryland 20899, United States;* orcid.org/0000-0002-3203-4833

Richard E. Gillilan − *Center for High-Energy X-ray Sciences at CHESS, Cornell University, Ithaca, New York 14853, United States*

Qingqiu Huang − *Center for High-Energy X-ray Sciences at CHESS, Cornell University, Ithaca, New York 14853, United States*

Harold W. Hatch − *Material Measurement Laboratory, National Institute of Standards and Technology, Gaithersburg, Maryland 20899, United States;* orcid.org/0000-0003-2926-9145

Vincent K. Shen − *Material Measurement Laboratory, National Institute of Standards and Technology, Gaithersburg, Maryland 20899, United States*

Alexander V. Grishaev − *Material Measurement Laboratory, National Institute of Standards and Technology, Gaithersburg, Maryland 20899, United States;* orcid.org/0000-0002-9347-2327

Suzette Pabit − *Analytical Enabling Capabilities, Merck & Co., Inc., Rahway, New Jersey 07065, United States*

Rahul Upadhya − *Analytical Enabling Capabilities, Merck & Co., Inc., Rahway, New Jersey 07065, United States*

Sudeep Adhikari − *Analytical Enabling Capabilities, Merck & Co., Inc., Rahway, New Jersey 07065, United States*

Complete contact information is available at:
https://pubs.acs.org/10.1021/acs.molpharmaceut.4c00460

Notes

The authors declare no competing financial interest.

■ ACKNOWLEDGMENTS

Certain commercial equipment, instruments, or materials (or suppliers, software, ...) are identified in this paper to foster understanding. Such identification does not imply recommendation or endorsement by the National Institute of Standards and Technology nor does it imply that the materials or equipment identified are necessarily the best available for the purpose. This work is based on research conducted at the Center for High-Energy X-ray Sciences (CHEXS), which is supported by the National Science Foundation (BIO, ENG and MPS Directorates) under award DMR-1829070, and the Macromolecular Diffraction at CHESS (MacCHESS) facility, which is supported by award 1-P30-GM124166-01A1 from the National Institute of General Medical Sciences, National Institutes of Health, and by New York State's Empire State Development Corporation (NYSTAR). Y.L. acknowledges the support provided by the Center for High Resolution Neutron Scattering, a partnership between the National Institute of Standards and Technology and the National Science Foundation under agreement no. DMR-2010792.

■ REFERENCES

(1) Rajewsky, K. The advent and rise of monoclonal antibodies. *Nature* **2019**, *575* (7781), 47−49.

(2) Shire, S. *Monoclonal Antibodies*; Elsevier, 2015.

(3) Yadav, S.; Shire, S. J.; Kalonia, D. S. Factors Affecting the Viscosity in High Concentration Solutions of Different Monoclonal Antibodies. *J. Pharm. Sci.* **2010**, *99* (12), 4812−4829.

(4) Zhang, Z. H.; Liu, Y. Recent progresses of understanding the viscosity of concentrated protein solutions. *Curr. Opin. Chem. Eng.* **2017**, *16*, 48−55.

(5) Yadav, S.; Laue, T. M.; Kalonia, D. S.; Singh, S. N.; Shire, S. J. The Influence of Charge Distribution on Self-Association and Viscosity Behavior of Monoclonal Antibody Solutions. *Mol. Pharm.* **2012**, *9* (4), 791−802.

(6) Li, L.; Kumar, S.; Buck, P. M.; Burns, C.; Lavoie, J.; Singh, S. K.; Warne, N. W.; Nichols, P.; Luksha, N.; Boardman, D. Concentration Dependent Viscosity of Monoclonal Antibody Solutions: Explaining Experimental Behavior in Terms of Molecular Properties. *Pharm. Res.* **2014**, *31* (11), 3161−3178.

(7) Chari, R.; Jerath, K.; Badkar, A. V.; Kalonia, D. S. Long- and Short-Range Electrostatic Interactions Affect the Rheology of Highly Concentrated Antibody Solutions. *Pharm. Res.* **2009**, *26* (12), 2607−2618.

(8) Lai, P. K.; Fernando, A.; Cloutier, T. K.; Gokarn, Y.; Zhang, J. F.; Schwenger, W.; Chari, R.; Calero-Rubio, C.; Trout, B. L. Machine Learning Applied to Determine the Molecular Descriptors Responsible for the Viscosity Behavior of Concentrated Therapeutic Antibodies. *Mol. Pharm.* **2021**, *18* (3), 1167−1175.

(9) Hong, T.; Iwashita, K.; Shiraki, K. Viscosity Control of Protein Solution by Small Solutes: A Review. *Curr. Protein Pept. Sci.* **2018**, *19* (8), 746−758.

(10) Guo, Z.; Chen, A.; Nassar, R.; Helk, B.; Mueller, C.; Tang, Y.; Gupta, K.; Klibanov, A. Structure-Activity Relationship for Hydrophobic Salts as Viscosity-Lowering Excipients for Concentrated Solutions of Monoclonal Antibodies. *Pharm. Res.* **2012**, *29* (11), 3102−3109.

(11) He, F.; Woods, C. E.; Litowski, J. R.; Roschen, L. A.; Gadgil, H. S.; Razinkov, V. I.; Kerwin, B. A. Effect of Sugar Molecules on the Viscosity of High Concentration Monoclonal Antibody Solutions. *Pharm. Res.* **2011**, *28* (7), 1552−1560.

(12) Wang, S. J.; Zhang, N.; Hu, T.; Dai, W. G.; Feng, X. Y.; Zhang, X. Y.; Qian, F. Viscosity-Lowering Effect of Amino Acids and Salts on Highly Concentrated Solutions of Two IgG1 Monoclonal Antibodies. *Mol. Pharm.* **2015**, *12* (12), 4478−4487.

(13) Xu, A. Y.; Castellanos, M. M.; Mattison, K.; Krueger, S.; Curtis, J. E. Studying Excipient Modulated Physical Stability and Viscosity of Monoclonal Antibody Formulations Using Small-Angle Scattering. *Mol. Pharm.* **2019**, *16* (10), 4319−4338.

(14) Chowdhury, A. A.; Manohar, N.; Lanzaro, A.; Kimball, W. D.; Witek, M. A.; Woldeyes, M. A.; Majumdar, R.; Qian, K. K.; Xu, S. F.; Gillilan, R. E.; et al. Characterizing Protein-Protein Interactions and Viscosity of a Monoclonal Antibody from Low to High Concentration Using Small-Angle X-ray Scattering and Molecular Dynamics Simulations. *Mol. Pharm.* **2023**, *20* (11), 5563−5578.

(15) Chowdhury, A.; Manohar, N.; Guruprasad, G.; Chen, A. T.; Lanzaro, A.; Blanco, M.; Johnston, K. P.; Truskett, T. M. Characterizing Experimental Monoclonal Antibody Interactions and Clustering Using a Coarse-Grained Simulation Library and a Viscosity Model. *J. Phys. Chem. B* **2023**, *127* (5), 1120−1137.

(16) Saito, S.; Hasegawa, J.; Kobayashi, N.; Kishi, N.; Uchiyama, S.; Fukui, K. Behavior of Monoclonal Antibodies: Relation Between the Second Virial Coefficient (B 2) at Low Concentrations and Aggregation Propensity and Viscosity at High Concentrations. *Pharm. Res.* **2012**, *29* (2), 397−410.

(17) Connolly, B. D.; Petry, C.; Yadav, S.; Demeule, B.; Ciaccio, N.; Moore, J. M. R.; Shire, S. J.; Gokarn, Y. R. Weak Interactions Govern the Viscosity of Concentrated Antibody Solutions: High-Throughput Analysis Using the Diffusion Interaction Parameter. *Biophys. J.* **2012**, *103* (1), 69−78.

(18) Kingsbury, J. S.; Saini, A.; Auclair, S. M.; Fu, L.; Lantz, M. M.; Halloran, K. T.; Calero-Rubio, C.; Schwenger, W.; Airiau, C. Y.; Zhang, J.; et al. A single molecular descriptor to predict solution behavior of therapeutic antibodies. *Sci. Adv.* **2020**, *6* (32), No. eabb0372.

(19) Neal, B. L.; Asthagiri, D.; Lenhoff, A. M. Molecular origins of osmotic second virial coefficients of proteins. *Biophys. J.* **1998**, *75* (5), 2469−2477.

(20) McBride, D. W.; Rodgers, V. G. J. Interpretation of negative second virial coefficients from non-attractive protein solution osmotic pressure data: An alternate perspective. *Biophys. Chem.* **2013**, *184*, 79−86.

(21) Wills, P. R.; Winzor, D. J. Rigorous analysis of static light scattering measurements on buffered protein solutions. *Biophys. Chem.* **2017**, *228*, 108−113.

(22) Blanco, M. A.; Sahin, E.; Li, Y.; Roberts, C. J. Reexamining protein-protein and protein-solvent interactions from Kirkwood-Buff analysis of light scattering in multi-component solutions. *J. Chem. Phys.* **2011**, *134* (22), 225103.

(23) Bonnete, F.; Malfois, M.; Finet, S.; Tardieu, A.; Lafont, S.; Veesler, S. Different tools to study interaction potentials in gamma-Crystallin solutions: Relevance to crystal growth. *Acta Crystallogr., Sect. D: Biol. Crystallogr.* **1997**, *53*, 438−447.
(24) Mrozowich, T.; Winzor, D. J.; Scott, D. J.; Patel, T. R. Experimental determination of second virial coefficients by small-angle X-ray scattering: a problem revisited. *Eur. Biophys. J. Biophys. Lett.* **2019**, *48* (8), 781−787.
(25) Receveur, V.; Durand, D.; Desmadril, M.; Calmettes, P. Repulsive interparticle interactions in a denatured protein solution revealed by small angle neutron scattering. *FEBS Lett.* **1998**, *426* (1), 57−61.
(26) Behlke, J.; Ristau, O. Analysis of the thermodynamic non-ideality of proteins by sedimentation equilibrium experiments. *Biophys. Chem.* **1999**, *76* (1), 13−23.
(27) Le Brun, V.; Friess, W.; Bassarab, S.; Mühlau, S.; Garidel, P. A critical evaluation of self-interaction chromatography as a predictive tool for the assessment of protein-protein interactions in protein formulation development: A case study of a therapeutic monoclonal antibody. *Eur. J. Pharm. Biopharm.* **2010**, *75* (1), 16−25.
(28) Winzor, D. J.; Wills, P. R. Allowance for thermodynamic non-ideality in the characterization of protein self-association by frontal exclusion chromatography: hemoglobin revisited. *Biophys. Chem.* **2003**, *104* (1), 345−359.
(29) Schmitz, K. S. *An Introduction to Dynamic Light Scattering by Macromoilecules*; Academic Press, 1990.
(30) Lehermayr, C.; Mahler, H.-C.; Mäder, K.; Fischer, S. Assessment of Net Charge and Protein-Protein Interactions of Different Monoclonal Antibodies. *J. Pharm. Sci.* **2011**, *100* (7), 2551−2562.
(31) Roberts, D.; Keeling, R.; Tracka, M.; van der Walle, C. F.; Uddin, S.; Warwicker, J.; Curtis, R. The Role of Electrostatics in Protein-Protein Interactions of a Monoclonal Antibody. *Mol. Pharm.* **2014**, *11* (7), 2475−2489.
(32) Woldeyes, M. A.; Qi, W.; Razinkov, V. I.; Furst, E. M.; Roberts, C. J. How Well Do Low- and High-Concentration Protein Interactions Predict Solution Viscosities of Monoclonal Antibodies? *J. Pharm. Sci.* **2019**, *108* (1), 142−154.
(33) Saito, S.; Hasegawa, J.; Kobayashi, N.; Tomitsuka, T.; Uchiyama, S.; Fukui, K. Effects of Ionic Strength and Sugars on the Aggregation Propensity of Monoclonal Antibodies: Influence of Colloidal and Conformational Stabilities. *Pharm. Res.* **2013**, *30* (5), 1263−1280.
(34) Liu, J.; Nguyen, M. D. H.; Andya, J. D.; Shire, S. J. Reversible self-association increases the viscosity of a concentrated monoclonal antibody in aqueous solution. *J. Pharm. Sci.* **2005**, *94* (9), 1928−1940.
(35) Yearley, E. J.; Godfrin, P. D.; Perevozchikova, T.; Zhang, H. L.; Falus, P.; Porcar, L.; Nagao, M.; Curtis, J. E.; Gawande, P.; Taing, R.; et al. Observation of Small Cluster Formation in Concentrated Monoclonal Antibody Solutions and Its Implications to Solution Viscosity. *Biophys. J.* **2014**, *106* (8), 1763−1770.
(36) Godfrin, P. D.; Zarraga, I. E.; Zarzar, J.; Porcar, L.; Falus, P.; Wagner, N. J.; Liu, Y. Effect of Hierarchical Cluster Formation on the Viscosity of Concentrated Monoclonal Antibody Formulations Studied by Neutron Scattering. *J. Phys. Chem. B* **2016**, *120* (2), 278−291.
(37) Godfrin, P. D.; Hudson, S. D.; Hong, K.; Porcar, L.; Falus, P.; Wagner, N. J.; Liu, Y. Short-Time Glassy Dynamics in Viscous Protein Solutions with Competing Interactions. *Phys. Rev. Lett.* **2015**, *115* (22), 228302.
(38) Hung, J. J.; Dear, B. J.; Karouta, C. A.; Chowdhury, A. A.; Godfrin, P. D.; Bollinger, J. A.; Nieto, M. P.; Wilks, L. R.; Shay, T. Y.; Ramachandran, K.; et al. Protein-Protein Interactions of Highly Concentrated Monoclonal Antibody Solutions via Static Light Scattering and Influence on the Viscosity. *J. Phys. Chem. B* **2019**, *123* (4), 739−755.
(39) Dear, B.; Hung, J. J.; Truskett, T. M.; Johnston, K. P. Contrasting the Influence of Cationic Amino Acids on the Viscosity and Stability of a Highly Concentrated Monoclonal Antibody. *Pharm. Res.* **2017**, *34* (1), 193−207.
(40) Dear, B. J.; Hung, J. J.; Laber, J. R.; Wilks, L. R.; Sharma, A.; Truskett, T. M.; Johnston, K. P. Enhancing Stability and Reducing Viscosity of a Monoclonal Antibody With Cosolutes by Weakening Protein-Protein Interactions. *J. Pharm. Sci.* **2019**, *108* (8), 2517−2526.
(41) Binabaji, E.; Ma, J. F.; Zydney, A. L. Intermolecular Interactions and the Viscosity of Highly Concentrated Monoclonal Antibody Solutions. *Pharm. Res.* **2015**, *32* (9), 3102−3109.
(42) Baek, Y.; Singh, N.; Arunkumar, A.; Zydney, A. L. Effects of Histidine and Sucrose on the Biophysical Properties of a Monoclonal Antibody. *Pharm. Res.* **2017**, *34* (3), 629−639.
(43) Valente, J. J.; Payne, R. W.; Manning, M. C.; Wilson, W. W.; Henry, C. S. Colloidal behavior of proteins: Effects of the second virial coefficient on solubility, crystallization and aggregation of proteins in aqueous solution. *Curr. Pharm. Biotechnol.* **2005**, *6* (6), 427−436.
(44) Rubin, J.; Linden, L.; Coco, W. M.; Bommarius, A. S.; Behrens, S. H. Salt-induced aggregation of a monoclonal human immunoglobulin G1. *J. Pharm. Sci.* **2013**, *102* (2), 377−386.
(45) Menzen, T.; Friess, W. Temperature-Ramped Studies on the Aggregation, Unfolding, and Interaction of a Therapeutic Monoclonal Antibody. *J. Pharm. Sci.* **2014**, *103* (2), 445−455.
(46) Antipova, A. S.; Semenova, M. G.; Belyakova, L. E. The effect of sucrose on the thermodynamic properties of ovalbumin and sodium caseinate in bulk solution and at air−water interface. *Colloids Surf., B* **1999**, *12*, 261−270.
(47) Woldeyes, M. A.; Qi, W.; Razinkov, V. I.; Furst, E. M.; Roberts, C. J. Temperature Dependence of Protein Solution Viscosity and Protein-Protein Interactions: Insights into the Origins of High-Viscosity Protein Solutions. *Mol. Pharm.* **2020**, *17* (12), 4473−4482.
(48) Hudson, S. D.; Sarangapani, P.; Pathak, J. A.; Migler, K. B. A Microliter Capillary Rheometer for Characterization of Protein Solutions. *J. Pharm. Sci.* **2015**, *104* (2), 678−685.
(49) Josephson, L. L.; Galush, W. J.; Furst, E. M. Parallel temperature-dependent microrheological measurements in a microfluidic chip. *Biomicrofluidics* **2016**, *10* (4), 043503.
(50) Monkos, K. Concentration and temperature dependence of viscosity in lysozyme aqueous solutions. *Biochim. Biophys. Acta, Protein Struct. Mol. Enzymol.* **1997**, *1339* (2), 304−310.
(51) Monkos, K.; Turczynski, B. A comparative study on viscosity of human, bovine and pig IgG immunoglobulins in aqueous solutions. *Int. J. Biol. Macromol.* **1999**, *26*, 155−159.
(52) Lee, J. C.; Timasheff, S. N. The Stabilization of Proteins by Sucrose. *J. Biol. Chem.* **1981**, *256* (14), 7193−7201.
(53) Timasheff, S. N. The Control of Protein Stability and Association by Weak-Interactions with Water - How Do Solvents Affect These Processes. *Annu. Rev. Biophys. Biomol. Struct.* **1993**, *22*, 67−97.
(54) Salipante, P. F.; Kuei, S.; Hudson, S. D. A small-volume microcapillary rheometer. *Rheol. Acta* **2022**, *61*, 309−317.
(55) Kestin, J.; Khalifa, H. E.; Correia, R. J. Tables of the Dynamic and Kinematic Viscosity of Aqueous NaCl Solutions in the Temperature-Range 20−150 °C and the Pressure Range 0.1−35 MPa. *J. Phys. Chem. Ref. Data* **1981**, *10* (1), 71−88.
(56) Telis, V. R. N.; Telis-Romero, J.; Mazzotti, H. B.; Gabas, A. L. Viscosity of aqueous carbohydrate solutions at different temperatures and concentrations. *Int. J. Food Prop.* **2007**, *10* (1), 185−195.
(57) Schiebener, P.; Straub, J.; Sengers, J. M. H. L.; Gallagher, J. S. Refractive-Index of Water and Steam as Function of Wavelength, Temperature and Density. *J. Phys. Chem. Ref. Data* **1990**, *19* (3), 677−717.
(58) Hopkins, J. B.; Gillilan, R. E.; Skou, S. *BioXTAS RAW*: improvements to a free open-source program for small-angle X-ray scattering data reduction and analysis. *J. Appl. Crystallogr.* **2017**, *50*, 1545−1553.
(59) Guinier, A.; Fournet, G. *Small-Angle Scattering of X-Rays*; John Wiley & Sons, Inc, 1955.

(60) Higgins, J. S.; Benoît, H. *Polymers and Neutron Scattering*; Clarendon Press, 1994.
(61) Cloutier, T.; Sudrik, C.; Mody, N.; Sathish, H. A.; Trout, B. L. Molecular Computations of Preferential Interaction Coefficients of IgG1 Monoclonal Antibodies with Sorbitol, Sucrose, and Trehalose and the Impact of These Excipients on Aggregation and Viscosity. *Mol. Pharm.* **2019**, *16* (8), 3657−3664.
(62) Moore, W. R.; Brown, A. M. Viscosity-Temperature Relationships for Dilute Solutions of Cellulose Derivatives: I. Temperature Dependence of Solution Viscosities of Ethyl Cellulose. *J. Colloid Sci.* **1959**, *14*, 1−12.
(63) Moore, W. R. Viscosity-Temperature Relationships for Dilute Solutions of High Polymers. *Nature* **1961**, *191* (4795), 1292−1293.
(64) Sorret, L. L.; DeWinter, M. A.; Schwartz, D. K.; Randolph, T. W. Challenges in Predicting Protein-Protein Interactions from Measurements of Molecular Diffusivity. *Biophys. J.* **2016**, *111* (9), 1831−1842.
(65) Shen, V. K.; Cheung, J. K.; Errington, J. R.; Truskett, T. M. Coarse-grained strategy for modeling protein stability in concentrated solutions. II: Phase behavior. *Biophys. J.* **2006**, *90* (6), 1949−1960.
(66) Nagele, G. On the dynamics and structure of charge-stabilized suspensions. *Phys. Rep.* **1996**, *272* (5−6), 215−372.
(67) Genz, U.; Klein, R. Collective Diffusion of Charged Spheres in the Presence of Hydrodynamic Interaction. *Physica A* **1991**, *171* (1), 26−42.
(68) Beenakker, C. W. J.; Mazur, P. Diffusion of spheres in a concentrated suspension II. *Physica A* **1984**, *126* (3), 349−370.
(69) Banchio, A. J.; Nägele, G. Short-time transport properties in dense suspensions: From neutral to charge-stabilized colloidal spheres. *J. Chem. Phys.* **2008**, *128* (10), 104903.
(70) Porcar, L.; Falus, P.; Chen, W. R.; Faraone, A.; Fratini, E.; Hong, K. L.; Baglioni, P.; Liu, Y. Formation of the Dynamic Clusters in Concentrated Lysozyme Protein Solutions. *J. Phys. Chem. Lett.* **2010**, *1* (1), 126−129.
(71) Jones, R. B.; Pusey, P. N. Dynamics of Suspended Colloidal Spheres. *Annu. Rev. Phys. Chem.* **1991**, *42*, 137−169.
(72) Roberts, C. J.; Blanco, M. A. Role of Anisotropic Interactions for Proteins and Patchy Nanoparticles. *J. Phys. Chem. B* **2014**, *118* (44), 12599−12611.

https://doi.org/10.1021/acs.molpharmaceut.4c00460
Mol. Pharmaceutics 2024, 21, 4553−4564